Fracture Mechanics of Concrete and Concrete Structures -
Assessment, Durability, Monitoring and Retrofitting of Concrete Structures- B. H. Oh, et al. (eds)
ⓒ 2010 Korea Concrete Institute, Seoul, ISBN 978-89-5708-181-5

Debonding condition monitoring of a CFRP laminated concrete beam using piezoelectric impedance sensor nodes

S. Park & S.-K. Park
Department of u-City Design and Engineering, Sungkyunkwan Univ, Suwon, Gyeonggi 440-746, Korea
Department of Civil and Environmental Engineering, Sungkyunkwan Univ, Suwon, Gyeonggi 440-746, Korea

J.-W. Kim & H.-J. Chang,
Department of u-City Design and Engineering, Sungkyunkwan Univ, Suwon, Gyeonggi 440-746, Korea

ABSTRACT: Carbon fiber reinforced polymer (CFRP) laminated concrete structures are used widely in a range of engineering fields because of their many advantages. However they always carry the risk of structural collapse initiated from the debonding conditions that might occur between the CFRP and concrete surface. This study employed an electro-mechanical impedance-based wireless structural health monitoring (SHM) technique by applying PZT ceramic patches to identify the debonding conditions of a CFRP laminated reinforced concrete beam. In the experimental study, the CFRP-reinforced concrete specimens were fabricated and the impedance signals were measured from the wireless impedance sensor node according to the different debonding conditions between the concrete and CFRP. Cross correlation (CC)-based data analysis was conducted to quantify the changes in impedance measured at the PZT patches due to the debonding conditions. The results confirmed that an impedance-based wireless SHM technique can be used effectively for monitoring the debonding of CFRP laminated concrete structures.

1 INTRODUCTION

In the 21st century, many larger, higher and more advanced building and bridge structures are being constructed with more complex systems. In addition, retrofitting and/or strengthening facilities are being added to existing critical civil infrastructure to deal with the effects of aging . Therefore, the construction, reinforcement and maintenance of the civil infrastructures are becoming increasingly important. In many types of reinforcements and maintenance methods, the use of the CFRP (Carbon Fiber reinforced polymer) reinforcement displayed in Figure 1 has increased steadily since 1992. A CFRP plate is made by mixing carbon fibers toward a certain direction. CFRP reinforcing is a reinforcement and maintenance method that involves attaching a CFRP plate to epoxy resin to recover and improve the physical performance of existing RC structures. CFRP has an ultimate strength more than five times that of steel and is less than 60% of the weight of aluminum. Therefore, the increase in load is small when it is used. In addition, it can provide effective waterproofing to damaged concrete and help prevent the corrosion of steel on account of its good chemical and water resistance. This method can also be applied to shorten the construction period and give higher reliability than the steel plate reinforcing method. However, this method is deficient in strength and reliability on the bonded area. The health of CFRP-reinforced RC structures is often controlled

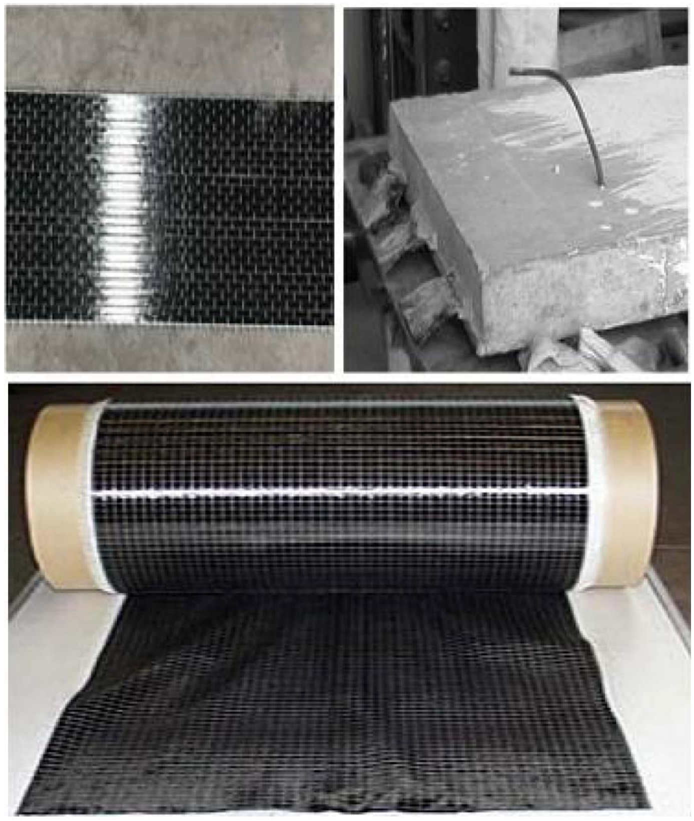

Figure 1. Carbon fiber reinforced polymer (CFRP).

by the condition of the attachment between the CFRP sheets and concrete. A FRP-attached concrete structure has high probability of attachment destruction before bending and shear failure. Therefore, predicting the destruction of FRP attachment is very important (Kim *et al.* 2008). This experimental study monitored the CFRP debonding condition using the impedance-based damage detection technique, which employs PZT (Lead-Zirconate-Titanate) sensors. Nowadays, SHM (structural health monitoring) is becoming increasingly important because natural disasters, environmental effects, such as temperature changes, impact loading and other deteriorating conditions, affect the strength and the serviceability of civil infrastructures. In particular, there is in increasing interest in monitoring the health of critical civil infrastructure. Even minor incipient damage to critical members in civil infrastructure can lead to failure that could cause a catastrophic accident. There have been many collapse accidents in civil infrastructure over the past two decades. It was found that these accidents were initiated from local failure of the critical members. A range of SHM and/or NDE (nondestructive evaluation) techniques such as acceleration-based modal testing, x-ray inspection and ultrasonic inspection have been used to prevent failure of the critical members in advance. However, these conventional SHM/NDE systems require complex algorithms or bulky and expensive equipment, which is not attractive for real applications. Recently, the electromechanical impedance-based damage detection technique was found to be a very powerful and innovative tool for detecting local damage in a variety of structures (Giurgiutiu *et al.* 1999, Park *et al.* 2000, 2003, Tseng *et al.* 2000, Zagrai and Giurgiutiu 2001, Park *et al.* 2005, 2006, 2007). In this study, a PZT sensor was used to detect electromechanical impedance-based damage. PZT sensors acting in a 'direct' manner produce an electrical charge when stressed mechanically. On the other hand, mechanical strain is produced when an electrical field is applied. The direct piezoelectric effect is often used in sensors, such as a piezoelectric accelerometer. With the converse effect, piezoelectric materials apply localized strain and affect the dynamic response of the structural elements directly when either embedded or surface bonded to a structure. PZT sensors are used widely in structural dynamics applications because they are lightweight, robust, inexpensive and can be purchased in a variety of forms ranging from thin rectangular patches to complex shapes for use in MEMS fabrication. The applications of piezoelectric materials in structural dynamics are too numerous to mention and are detailed in literature. (Niezrecki *et al.* 2001, Chopra 2002). The main goal of this study was to evaluate the impedance-based SHM technique for CFRP debonding monitoring throughout a series of experimental studies. Firstly, a CFRP reinforced concrete specimen was fabricated and two PZT sensors were attached to the surface of the CFRP. Different conditions of CFRP attachment with perfect bonding, and 2cm, 4cm and 6cm debonding conditions were examined in sequence and wireless impedance measurements are taken according to each step using the impedance sensor node.

2 THEORETICAL BACKGROUNDS

2.1 *Electromechanical Impedance-based SHM Techniques*

The E/M impedance-based SHM techniques employ small piezoelectric sensors attached to simultaneously excite the structure with a high-frequency, and monitor the changes in the E/M impedance signature. In addition, the self-sensing properties allow one piece of piezoelectric material to sense the input voltage and output current. When the PZT patch is surface-bonded to a host structure, Liang *et al.* (1994) reported that the electrical admittance (inverse of the electrical impedance), $Y(\omega)$, of a PZT patch is associated with the mechanical impedance of the host structure, $Z_s(\omega)$, and that of a PZT patch, $Z_a(\omega)$ through Equation (1):

$$Y(\omega) = j\omega \frac{wl}{h}\{\bar{\varepsilon}_{33}^{T} - d_{31}^{2}\bar{Y}^{E} + (\frac{Z_a(\omega)}{Z_s(\omega)+Z_a(\omega)})d_{31}^{2}\bar{Y}^{E}(\frac{\tan \kappa l}{\kappa l})\} \quad (1)$$

where w, l and h are the width, length and thickness of a PZT patch, respectively, and $\bar{\varepsilon}_{33}^{T} = \varepsilon_{33}^{T}(1-\delta j)$ is the complex electric permittivity of a PZT patch at constant stress, respectively. δ denotes the dielectric loss factor of a PZT patch, $\bar{Y}^{E} = Y^{E}(1+\eta j)$ is the Yong's modulus of a PZT patch at a constant electric field, η denotes the mechanical loss factor of the PZT patch, d_{31} is the piezoelectric constant of a PZT patch, $Z_s(\omega)$ and $Z_a(\omega)$ are the electrical impedance of a PZT patch and host structure, respectively, $\kappa = \omega(\rho/\bar{Y}^{E})^{1/2}$ is the wave number and ρ is the mass density of a PZT patch. It should be noted that the measured admittance function, $Y(\omega)$, is a complex number that consists of a real and imaginary part, and can be readjusted, as shown in equation (2).

$$Y(\omega) = G(\omega) + jB(\omega) = j\omega C\left(1-\kappa_{31}^{2}\frac{Z_s(\omega)}{Z_s(\omega)+Z_a(\omega)}\right) \quad (2)$$

where G is the conductance (real part), B is the susceptance (imaginary part), C is the zero-load capacitance of the PZT, k_{31} is the electromechanical coupling coefficient of the PZT. Bhalla *et al.*(2002) reported that the real part of the measured admittance can be changed more sensitively depending on the extent of structural damage than the imaginary parts, whereas Park *et al.* (2009) showed that the imaginary parts can be used more effectively for piezoelectric sensor self-diagnosis.

2.2 *Statistical damage metric: RMSD and correlation coefficient*

Assessments of the integrity of the mechanical structure can be made by observing some of the changes in the E/M impedance of the PZT. While impedance changes provide a qualitative assessment of the extent of damage, a quantitative measure of damage is made traditionally using a scalar damage metric, which is referred to as root mean square deviation (RMSD) as follows:

$$RMSD(\%) = \sqrt{\frac{\sum_{i=1}^{n}\{\mathrm{Re}(Z_{i,1}) - \mathrm{Re}(Z_{i,0})\}^2}{\sum_{i=1}^{n}\{\mathrm{Re}(Z_{i,0})\}^2}} \times 100 \qquad (3)$$

where Z_{i0} is the impedance of the PZT measured in the healthy condition (baseline), Z_{i1} is the impedance of the concurrent condition, and n is the number of frequency points. In a RMSD chart, a larger numerical value of the metric means a larger difference between the baseline reading and subsequent reading indicating the presence of damage in a structure. Temperature variations due to the surrounding changes would be nonexistent because they would result in a significant change in impedance, particularly a frequency shift in the impedance, which may lead to erroneous diagnostic results of a real structure. However, it is a difficult and inevitable problem that needs to be overcome by engineers. Recently, several studies reported the effects of temperature variations on the impedance measurement (Bhalla *et al.* 2002, Koo *et al.* 2009). Bhalla *et al.* (2002) examined the influence of the structure-actuator interactions and temperature on the impedance signatures. Koo *et al.* (2009) proposed the effective frequency shift (EFS), $\overline{\omega}$, based on the maximum cross correlation coefficient between the reference impedance data, $x(\omega)$, and the concurrent impedance data, $y(\omega)$ as follows:

$$\max_{\tilde{\omega}} CC = \max_{\tilde{\omega}}\{\frac{1}{N}\sum_{i=1}^{n}(x(\omega_i) - \bar{x})(y(\omega_i - \tilde{\omega}) - \bar{y})\} \Big/ \sigma_X \, \sigma_Y \qquad (4)$$

where x and y are the mean values of the impedance signals of $x(\omega)$ and $y(\omega)$, respectively, and σ_x and σ_Y are the standard deviations for each. Since the cross-correlation metric accounts for the vertical and horizontal shifts of the impedance signatures normally associated with the changes in temperature, the proposed EFS-based damage metric presents the temperature compensation effects on the impedance measurements.

2.3 *Wireless sensor nodes for impedance-based structural health monitoring*

In this study, the impedance data was collected using a wireless impedance sensor node developed recently by KAIST and the Korea Electronics Technology Institute (KETI) (Min *et al.* 2009). This wireless sensor node consists of three functional subsystems: (1) sensing interface, (2) computational core, and (3) wireless transceiver. The sensing interface includes an interface to which a piezoelectric sensor and/or a temperature sensor (NTC-10KD-5J type) can be connected and an impedance chip (AD5933) to excite the piezoelectric sensor and measure the impedance signals. The computational core consists of a microcontroller (ATmega128L) for computational tasks and a flash memory with software programs for system operation and data processing. The wireless transceiver is an integral component of the wireless system, which is composed of a RF module (CC2420) and antenna to communicate processing information with other wireless sensor nodes and/or transferring the processed data to the server. For a continuous SHM using a wireless sensor node, it is important to construct signal processing algorithms to identify the damage in microcontroller (ATmega128L). The pre-described algorithms for calculating the statistical damage metric (RMSD and cross-correlation coefficient) are embedded on the sensor node. Therefore, the user instantly receives both the processed and raw data. In addition, the server sends an alarm to the administrator if the damage metric is out of the pre-decided safe range. The strongest point of the sensor node is that it can compensate for the effect of temperature on the E/M impedance data and calculate the damage metric on the microcontroller. Figures 2 and 3 show a prototype of the wireless impedance sensor node and its block diagram, respectively.

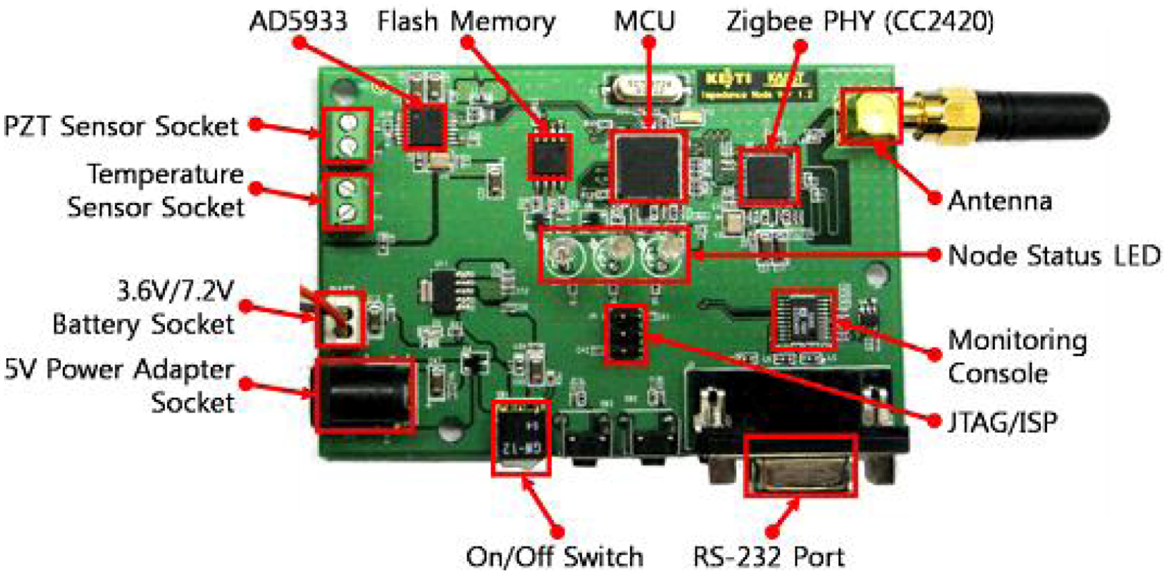

Figure 2. Wireless impedance sensor node (Min *et* al 2009).

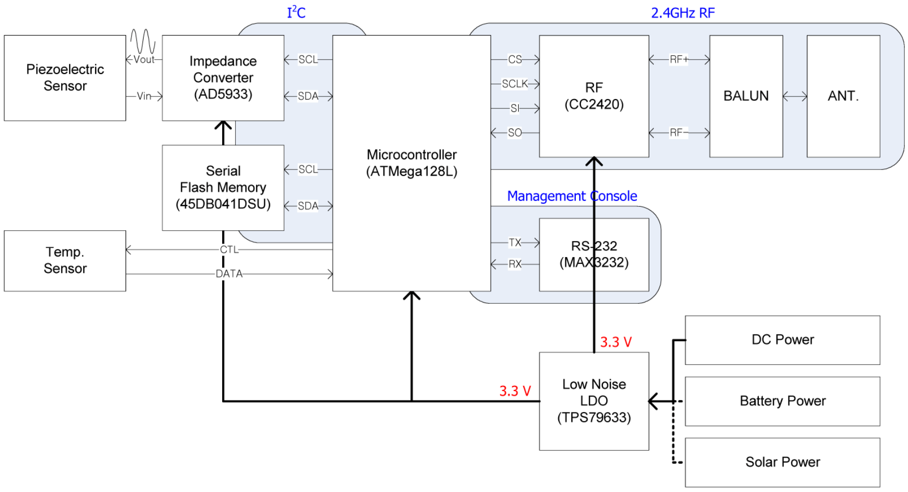

Figure 3. Block diagram of sensor node.

3 EXPERIMENTAL STUDIES

3.1 *Experimental setup*

A series of experimental studies was carried out to examine the capability of the impedance-based SHM technique for CFRP debonding monitoring. As shown in Figure 4, a reinforced concrete specimen, 40 cm long, 10 cm wide and 10 cm thick, was prepared and a CFRP, 30 cm long, 5 cm wide and 3 mm thick, was attached to the bottom of the reinforced concrete specimen. Two PZT patch-type sensors (PZTs #1 and #2), 3.6cm x 3.6cm x 0.05cm, were bonded to the surface of the CFRP with super glue. PZT #1 and #2 were 10cm and 20cm away from the right-end of CFRP, respectively. The PZT patches are used as both actuators and sensors simultaneously. A PZT patch simultaneously performs both roles of a transmitter, which sends the signal, and receiver, which receives the signal, at the same time. The measured impedance signals are sent to a RF receiver connected to a laptop computer through the wireless impedance

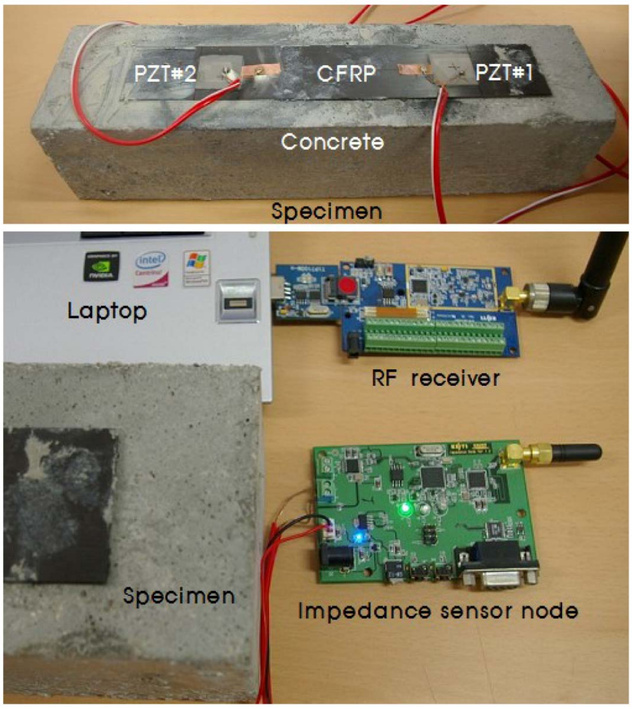

Figure 4. Experimental setun.

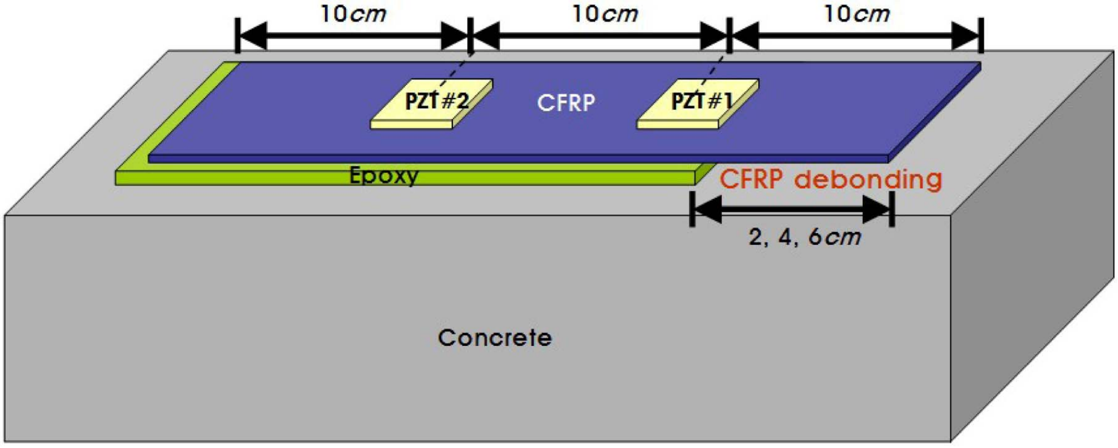

Figure 5. Test specimen: A CFRP laminated concrete.

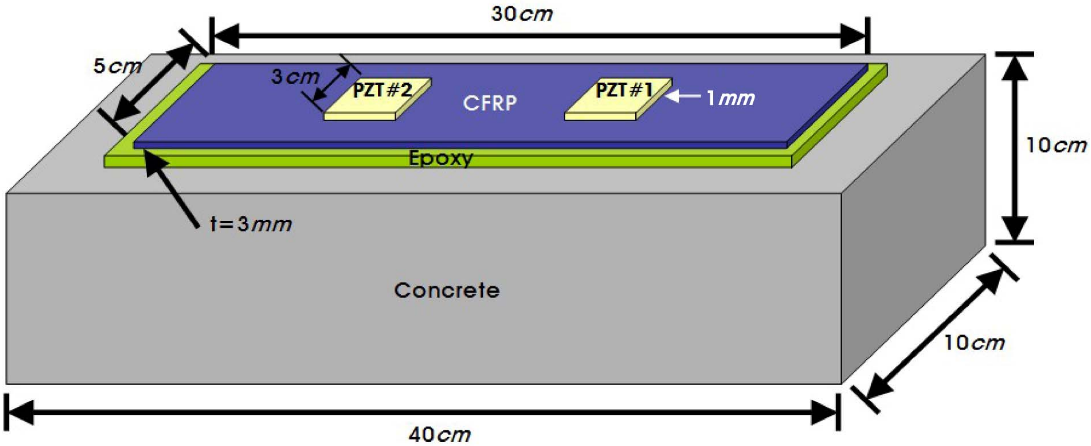

Figure 6. Test specimen with CFRP debonding condition.

sensor node. The impedance signals were measured 5 times over the frequency range of 1 kHz ~ 3 kHz and averaged to reduce the S/N ratio of the impedance data. This frequency range was chosen because it contains a good dynamic interaction between the PZT and structure with multiple resonant peaks. To examine the effects of CFRP debonding, different conditions of the CFRP bonding with perfect bonding, and 2cm, 4cm and 6cm debonding conditions were investigated in sequence and the impedance measurements were performed in real-time according to each step, as shown in Figures 5 and 6.

3.2 *Experimental result*

The real-time impedance signals were measured at both PZTs #1 and #2 according to the different debonding conditions with 2cm, 4cm and 6cm debonding between the CFRP and concrete surface. Figures 7 and 8 show the impedance data obtained from PZTs #1 and #2, respectively. In the right of Figures 7 and 8, the frequency range of 2.35 kHz ~ 2.45 kHz was zoomed in to examine the impedance changes more clearly. In that figure, the change in the resonant frequency of the measured impedance signal increased with increasing CFRP debonding area.

Moreover, a comparison of Figure 7 with Figure 8 showed that PZT #1, which was located closer to the debonding spot, responded more sensitively to the debonding conditions than PZT #2, which was located further from the debonding spot, by showing larger shifts in the resonant frequency of the measured impedance data according to the increase in debonding. A cross correlation coefficients (CC)-based damage metric of Equation (4) was calculated to quantify the changes in the measured impedance data according to each debonding condition. Table 1 shows that as the CFRP debonding area increases from 0 cm to 2 cm, 4 cm and 6 cm, the CC-based damage metric increases as follows: 0, 0.15, 0.18 and 0.23 at PZT#1, respectively, and 0, 0.03, 0.05 and 0.07 at PZT#2, respectively. In addition, the rate of increase in the CC values is dependent on the location of the PZT sensors. When the max CC value of PZT#1's was 0.23 in the case of 6cm debonding, the max CC value of PZT#2 attached 10cm further away than PZT#1 was only 0.07. Figure 9 clearly shows the increase in max CC value and the change in the rates between PZT#1 and PZT#2. Overall, the impedance-based SHM technique using PZT sensors can be used effectively for wireless debonding monitoring of CFRP laminated concrete structures.

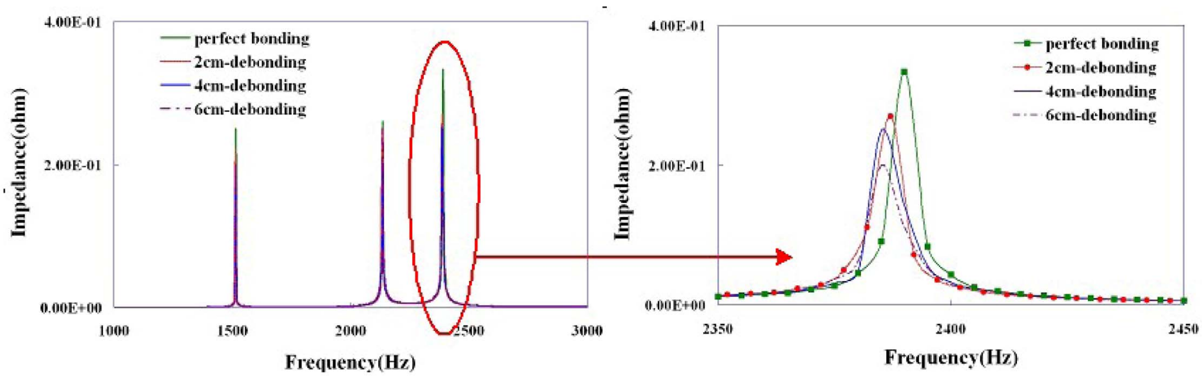

Figure 7. Changes in the impedance signatures measured at PZT#1.

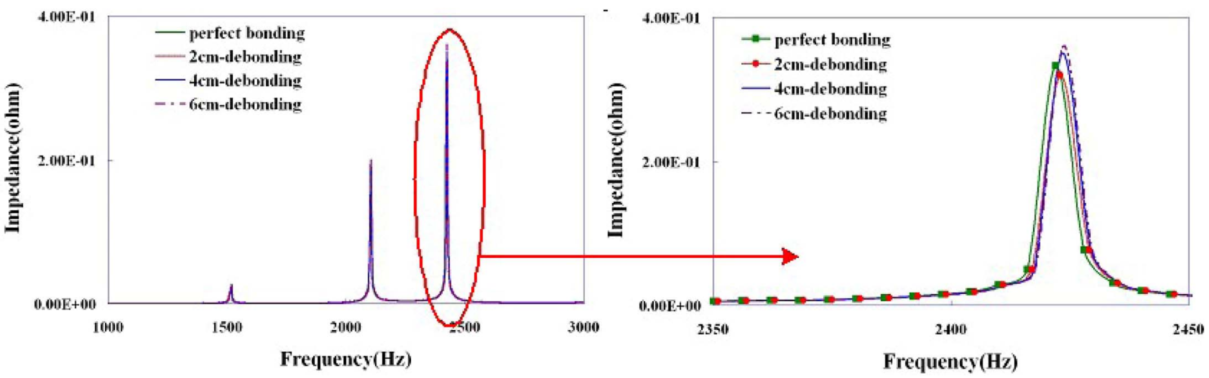

Figure 8. Changes in the impedance signatures measured at PZT#2.

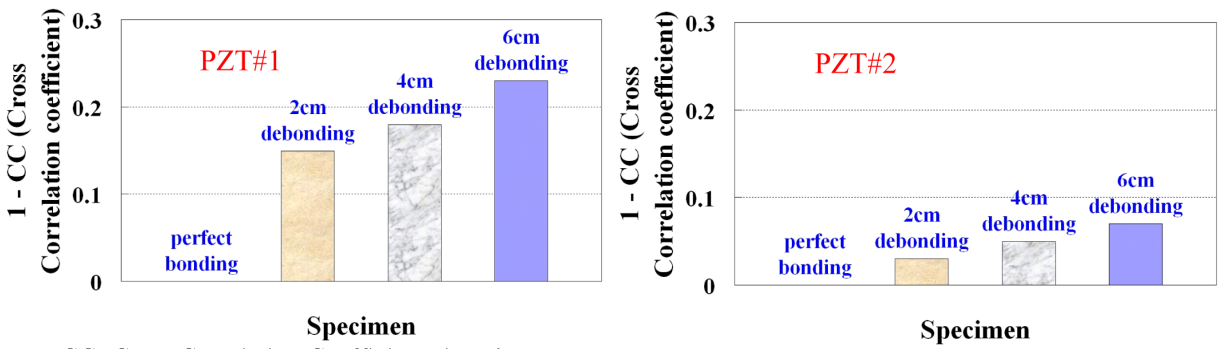

Figure 9. 1-CC (Cross Correlation Coefficient) bar chart.

Table 1. Damage index: 1-CC (Cross Correlation Coefficient).

PZT / Condition	1-CC (Cross Correlation Coefficient)	
	PZT#1	PZT#2
Perfect bonding	0	0
2cm debonding	0.15	0.03
4cm debon ding	0.18	0.05
6cm debonding	0.23	0.07

4 CONCLUSION

This study presented a new methodology for diagnosing the debonding condition of CFRP laminated concrete structures using PZT sensors. From the experimental study, the change in the impedance signal increased with increasing debonding. In addition, the PZT sensor located closer to the damaged area responded more sensitively to the debonding conditions than the PZT sensor located further away. Moreover, the changes in the impedance signatures according to the debonding conditions and the location of PZT sensor were evaluated using the CC (cross correlation) method as a statistical signal processing method. These results demonstrated that the impedance-based structural health monitoring (SHM) method can be used effectively to diagnose the debonding condition of CFRP laminated concrete structures.

ACKNOWLEDGMENT

This study was supported by the R&D(06 the core of construction B05) that was assigned by Korea Institute of Construction & Transportation Technology

Evaluation and Planning (KICTEP), Korea Land & Housing Corporation (LH) and u-City Master and Doctor support project funded by Ministry of Land, Transport and Maritime Affairs(MLTM). This all-out support is greatly appreciated.

REFERENCE

Bhalla, S., Naidu, A.S.K. and Soh, C.K. 2002. Influence of structure–actuator interactions and temperature on piezoelectric mechatronic signatures for NDE. *Proc. ISSS-SPIE 2002 International Conference on Smart Materials Structures and Systems.* 5062

Chopra, I. 2002. Review of state of art of smart structures and integrated systems. *AIAA Journal.* 20(11) : 2145-2187

Giurgiutiu, V., Reynolds, A. and Rogers, C.A. 1999. Experimental investigation of E/M impedance health monitoring of spot-welded structure joints. *Journal of Intelligent Material Systems and Structures.* 10(10):802-812

Kim, S.B., Kim, J.H., Nam, J.W., Kang, S.H. & Byeon, K.J. 2008. Bond-slip model of interface between CFRP sheets and concrete beams strengthened with CFRP, *Korea Concrete institute*, 20(4): 477-486

Koo K.Y., Park, S., Lee, J.-J. and Yun, C.-B. 2009. Automated impedance-based structural health monitoring Incorporating Effective Frequency Shift for Compensating Temperature Effects. *Journal of Intelligent Meterial Systems and Structures.* 20: 367-377

Liang, L., Sun, F.P. and Rogers, C.A. 1994. Coupled electro-mechanical analysis of adaptive material systems-determination of the actuator power consumption and system energy transfer. *Journal of Intelligent Material Systems and Structures.* 5:12-20

Min, J.Y., Park, S., Song, B.H. and Yun, C.-B. 2009. Development of wireless sensor nodes for impedance-based structural health monitoring. *The 6th international workshop on advanced smart materials and smart structures technology,ANCRiSST09, Boston, MA, USA, July 29-Aug 1.*

Niezrecki, C., Brei, D., Balakrishnan, S., Moskalik, A. 2001. Piezoelectric actuation: State of the art. *The Shock and Vibration Digest.* 33(4): 269-280

Park, G., Cudney, H. and Inman, D.J. 2000. Impedance-based health monitoring of civil structural components, *American Society of Civil Engineers*, 6(4):153-160

Park, G., Sohn, H., Farrar, C.R. and Inman, D.J. 2003. Overview of piezoelectric impedance-based health monitoring and path forward, *The Shock and Vibration Digest*, 35(6): 451-463

Park, S., Yun, C.B., Roh, Y. and Lee, J.J. 2005. Health monitoring of steel structures using impedance of thickness modes at PZT patches. *Smart Structures and Systems.* 1:339-53

Park S, Yun, C.B., Roh, Y. and Lee, J.J. 2006. PZT-based active damage detection techniques for steel bridge components. *Smart Materials and Structures.* 15: 957-966

Park, S., Grisso, B.L., Inman, D.J. and Yun, C.-B. 2007. MFC-based structural health monitoring using a miniaturized impedance measuring chip for corrosion detection. *Reserch in Nondestructive Evaluation. 18:139-150*

Park, S., Shin, H.-H. and Yun, C.-B. 2009. Wireless impedance sensor nodes for functions of structural damage identification and sensor self-diagnosis. *Smart Mater. Struct.* 18: 1-11.

Tseng, K.K., Soh, C.K., Gupta, A. and Bhalla, S. 2000. Health monitoring of civil infrastructures using smart piezoceramic transducers, *2nd International Conference on Computational Methodology for Smart Structures and Materials:* 153–162

Zagrai, A.N. and Giurgiutiu,V. 2001. Electro-mechanical impedance method for crack detection in thin wall structures. *3rd International Workshop on Structural Health Monitoring*